JOURNAL OF APPLIED ELECTROCHEMISTRY **25** (1995) 227–232

Preparation of solid polymer electrolyte composites: investigation of the ion-exchange process

P. MILLET

Laboratoire des Composés Non Stoechiométriques, Université de Paris-Sud, Bât. 415, 91405 Orsay Cedex, France

F. ANDOLFATTO, R. DURAND

Centre de Recherche en Electrochimie Minérale et en Génie des Procédés, BP 75, 38402 Saint-Martin d'Hères Cedex, France

Received 5 May 1994; revised 15 September 1994

The rate of ion-exchange between an aqueous solution of platinum tetramine and a Nafion® 117 membrane in H^+ form is studied. Experimental data are collected using extended X-ray absorption fine structure (EXAFS) spectroscopy in dispersive mode. Results are obtained for various platinum tetramine concentrations in the solution and different hydrodynamic regimes at the membrane–solution interface. A shift from a layer diffusion controlled rate (L) to a membrane diffusion controlled rate (M) is observed when the salt concentration and the stirring of the solution are increased. Time dependent fractional concentration in platinum tetramine inside the membrane are computed for the two limiting cases of diffusion (L and M). Good agreement is found between experimental and simulated data. The role of the rate of ion-exchange on the electrochemical performances of electrode–membrane–electrode composites for water electrolysis applications is discussed.

List of symbols

A	surface of the membrane contacting the solution ($1.0\,cm^2$)
A_{Pt}	geometrical area of the platinum RDE (cm^2)
C_i	concentration of species i in the bulk solution ($mol\,cm^{-3}$)
C_i^*	concentration of species i in the membrane ($mol\,cm^{-3}$)
C^-	sulfonate concentration in the membrane ($mol\,cm^{-3}$)
C_0	concentration at the membrane-solution interface ($mol\,cm^{-3}$)
D_i	diffusion coefficient of species i in the solution ($cm^2\,s^{-1}$)
D_i^*	diffusion coefficient of species i in the membrane ($cm^2\,s^{-1}$)
F	Faraday ($96\,500\,C\,mol^{-1}$)
I_L	limiting current of diffusion (A)
K	equilibrium constant $= C^*_{[Pt(NH_3)_4]^{2+}}/C_{[Pt(NH_3)_4]^{2+}}$ at equilibrium = 48 (298 K)
l	diffusion layer thickness (cm)
L	diameter of the cell (1.2 cm)
n	number of electron exchanged (2) during the electrooxidation of $[Pt(NH_3)_4]^{2+}$
N_i	fractional concentration of species i in the membrane $= z_i C_i^*/C^-$
Re	Reynolds number defined as vl/γ
Sc	Schmidt number defined as γ/D
$t_{1/2}$	time at which 50% of the ion-exchange is achieved
v	velocity of the solution ($cm\,s^{-1}$)
V	volume of the membrane ($0.01\,cm^3$)
z_i	charge beared by species i
γ	kinematic viscosity of the solution ($0.0114\,cm^2\,s^{-1}$) assumed to be equal to that of pure water at 298 K
δ	membrane thickness (cm)
ω	rotation speed of the RDE ($rad\,s^{-1}$)

1. Introduction

The preparation of noble-metal based Nafion® composites is of practical interest because of potential applications in solid polymer electrolyte (SPE®) water electrolysers and hydrogen/oxygen fuel cells [1, 2]. Such membrane–electrode assemblies (MEAs) can be prepared in different ways. For example, the coating under heat and/or pressure of a mixture of a catalyst powder and a binder on each side of the membrane [3, 4]; diffusion through the membrane of a reducing agent which reacts with an anionic salt of the metal to be plated [5].

Since the mid-1980s we have developed a procedure based on the localised chemical reduction of cationic noble-metal salts into Nafion® membranes. The platinum-based MEAs thus obtained show interesting electrochemical performance [6, 7]. The procedure consists of (i) ion-exchanging the membrane with platinum tetramine, and (ii) reducing *in situ* the platinum salt to the metallic state. The reduction process is achieved by immersing the platinum

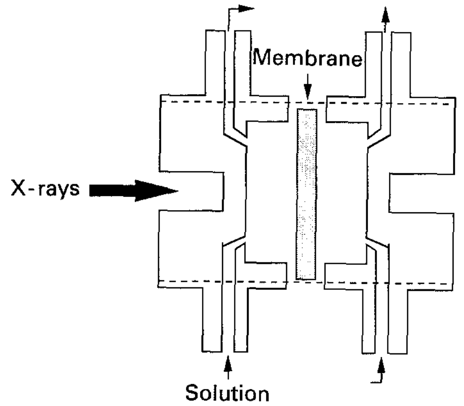

Fig. 1. Schematic diagram of the polyethylene cell used for the EXAFS experiments; cell dimensions: 4 cm × 4 cm × 2 cm; membrane dimensions: 2 cm × 2 cm × 0.019 cm.

tetramine-exchanged membrane in a reducing solution of sodium borohydride.

To optimize the electrochemical performance of the MEAs and to limit the amount of platinum deposited, we have studied *in situ* the ion-exchange and precipitation processes using EXAFS (extended X-ray absorption fine structure) spectroscopy in dispersive mode. Results [8] show that at low salt concentration in the solution and low stirring, the rate of ion-exchange is limited by ionic diffusion across the diffusion layer adherent to the membrane surface, whereas at higher salt concentration and with more efficient stirring, the rate becomes limited by the diffusion in the membrane itself. In this paper, we calculate the time variation of the platinum fractional concentration in the membrane by considering the two limiting cases of diffusion (layer and membrane limitation). The effect of the parameters controlling the rate of ion-exchange is discussed. Kinetic data presented in [8] are used to check the validity of the model. The precipitation process will be treated in a subsequent paper.

2. Experimental details

2.1. *Kinetic data*

Kinetic data were collected using EXAFS in dispersive mode [8]. The incorporation of platinum tetramine was followed *in situ* using the cell shown in Fig. 1. The concentration of the solutions was limited to 0.5 M because of the moderate solubility of the salt at room temperature. X-ray absorption by 0.5 M solutions (2 mm thick) was negligible, and the collected spectra were not corrected for the signal of the free solution.

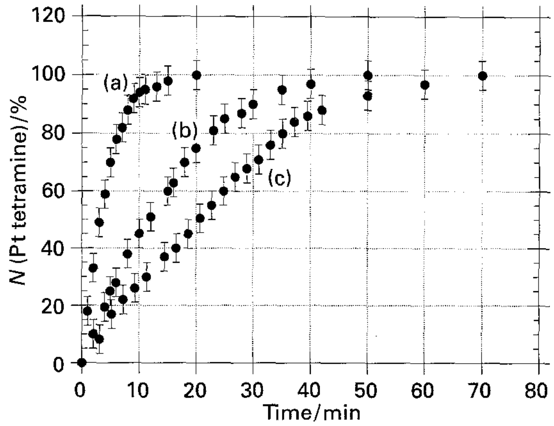

Fig. 2. $N_{[\mathrm{Pt(NH_3)_4}]^{2+}}$ (expressed in %) as a function of time; effect of the salt concentration in the solution: (a) $[\mathrm{Pt(NH_3)_4}]^{2+} = 3.75 \times 10^{-2}$ M; (b) $[\mathrm{Pt(NH_3)_4}]^{2+} = 10^{-2}$ M; $[\mathrm{Pt(NH_3)_4}]^{2+} = 5.5 \times 10^{-3}$ M; volume flow = 0.083 cm^3 s^{-1}.

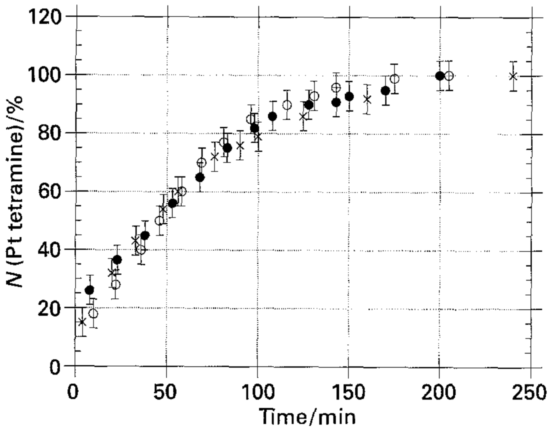

Fig. 3. $N_{[\mathrm{Pt(NH_3)_4}]^{2+}}$ (expressed in %) as a function of time; effect of the volume flow rate: (○) 0.35, (●) 0.7 and (×) 1.05 cm^3 s^{-1}. $[\mathrm{Pt(NH_3)_4}]^{2+}$ in the solution = 10^{-2} M.

The structure of the salt in the membrane was found to be $[\mathrm{Pt(NH_3)_4}]^{2+}$. Figure 2 shows the time variation of $N_{[\mathrm{Pt(NH_3)_4}]^{2+}}$ obtained for three different salt concentrations in the solution and under constant volume flow conditions across the cell. Figure 3 shows the time variation of $N_{[\mathrm{Pt(NH_3)_4}]^{2+}}$ obtained for three different regimes of stirring and at constant salt concentration in the solution.

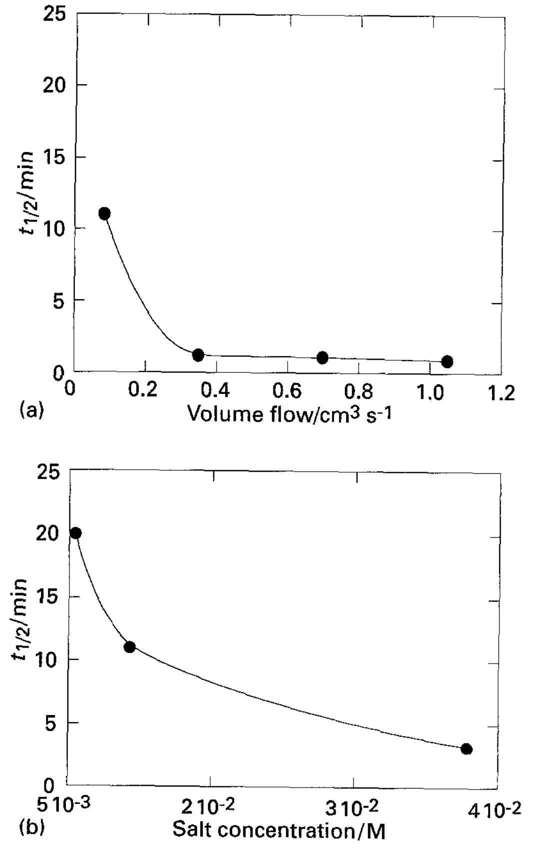

Fig. 4. Effect of (a) volume flow across the cell, and (b) salt concentration in the solution on the time for half-change. In (a) $[\mathrm{Pt(NH_3)_4}]^{2+} = 10^{-2}$ M; in (b) volume flow = 0.083 cm^3 s^{-1}.

From Fig. 4, the effect of the volume flow rate and the salt concentration in the solution on the time for half-change $t_{1/2}$ ($t_{1/2}$ is defined as the time at which 50% of the ion-exchange is achieved) can be seen.

2.2. *Diffusion coefficients*

The value of D_{H^+} in aqueous solution was taken from the literature [9] as $9 \times 10^{-5}\,\mathrm{cm^2\,s^{-1}}$ at room temperature.

According to Bard *et al.* [10], the anodic oxidation of platinum tetramine occurs as follows:

$$[\mathrm{Pt(NH_3)_4}]^{2+} + 2\,\mathrm{Cl}^- \longrightarrow [\mathrm{Pt(NH_3)_4Cl_2}]^{2+} + 2\mathrm{e}^-$$

The value of $D_{[\mathrm{Pt(NH_3)_4}]^{2+}}$ in aqueous solution was deduced from electrochemical measurements in aqueous solution using a platinum rotating disk electrode (RDE). Figure 5 shows the variation of the limiting current of oxidation of $[\mathrm{Pt(NH_3)_4}]^{2+}$ as a function of the square root of the rotation speed of the RDE. The measurements were made at 298 K in 0.5 M $\mathrm{H_2SO_4}$. The linear relationship between I_L and $\omega^{1/2}$ indicates that the kinetics of oxidation are limited by diffusion in the solution. $D_{[\mathrm{Pt(NH_3)_4}]^{2+}}$ was obtained from the following relation [11]:

$$I_\mathrm{L} = 0.62 nFA_\mathrm{Pt} C_{[\mathrm{Pt(NH_3)_4}]^{2+}} D^{2/3}_{[\mathrm{Pt(NH_3)_4}]^{2+}} \gamma^{-1/6} \omega^{1/2} \quad (1)$$

A value of $8.3 \times 10^{-6}\,\mathrm{cm^2\,s^{-1}}$ was obtained at room temperature.

$D^*_{H^+}$ and $D^*_{[\mathrm{Pt(NH_3)_4}]^{2+}}$ in the membrane were deduced from conductivity measurements as described elsewhere [12]. The following values were obtained:

$$D^*_{\mathrm{H}^+} = 2.3 \times 10^{-5}\,\mathrm{cm^2\,s^{-1}}$$

$$D^*_{[\mathrm{Pt(NH_3)_4}]^{2+}} = 5.2 \times 10^{-7}\,\mathrm{cm^2\,s^{-1}}$$

2.3. *Ion-exchange equilibrium constant*

The ion-exchange equilibrium constant K for $[\mathrm{Pt(NH_3)_4}]^{2+}$ was obtained as detailed elsewhere [13]. A value of 48 was obtained at room temperature.

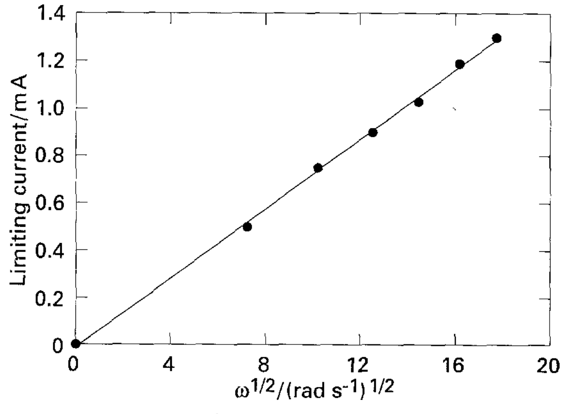

Fig. 5. Oxidation of 10^{-2} M $[\mathrm{Pt(NH_3)_4}]\,\mathrm{Cl_2}$ at a platinum RDE in $\mathrm{H_2SO_4}$ 0.5 M. The limiting current of oxidation I_L is plotted against $\omega^{1/2}$, the square root of the rotation speed of the electrode.

3. Theory

3.1. *Description of the model*

We consider the ion-exchange between an aqueous solution of platinum tetramine ($[\mathrm{Pt(NH_3)_4}]^{2+}$) and a Nafion® membrane in H^+ form at room temperature. As pointed out in [8], two limiting types of kinetics may be encountered: (i) diffusion in the boundary diffusion layer is rate-determining (L mechanism), (ii) diffusion in the membrane is rate-determining (M mechanism). It can be seen from Fig. 4 that the time for half-change $t_{1/2}$ becomes constant for values of the volume flow above ca. $0.35\,\mathrm{cm^3\,s^{-1}}$ and for values of the salt concentration above 0.05 M. A value of approximately 1 min is reached for $t_{1/2}$ in both cases. These results suggest a shift from L to M rate-determining mechanism when the salt concentration or the regime of stirring are increased. But as pointed out by Kressman and Kitchener [14], this criterion of constant $t_{1/2}$ is not conclusive. The rate may reach a limit for hydrodynamic reasons and it may still be possible to achieve faster rates of exchange by using a different type of stirrer. To check whether data of Fig. 4 correspond to a change in the mechanism controlling the rate of ion-exchange, $N_{[\mathrm{Pt(NH_3)_4}]^{2+}}$ was calculated as a function of time in the two limiting cases of mass transport.

The membrane–solution interface is represented in cross-section (Fig. 6). Three different zones can be distinguished: zone a, of infinite thickness, is the bulk solution; zone b, of thickness l, is the Nernst diffusion layer; zone c, of thickness $\delta/2$, is the Nafion® membrane.

3.2. *L mechanism*

We consider the simple case of the sorption of a diffusing species from a well-stirred solution. If the L mechanism is rate-controlling, then the rate of exchange satisfies the following differential equation:

$$\frac{\partial VC^*}{\partial t} = \frac{AD}{l}(C - C_0) = \frac{\partial VKC_0}{\partial t} \quad (2)$$

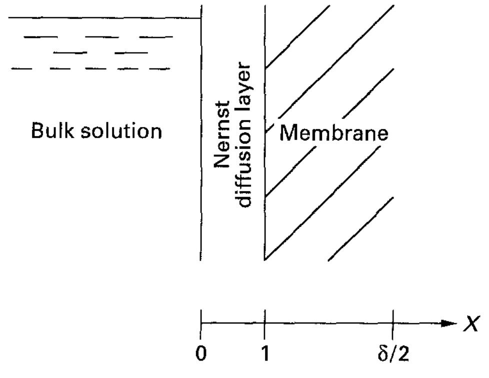

Fig. 6. Schematic diagram of the membrane–solution interface during the ion-exchange process.

The solution to Equation 2 is

$$C_0 = C - Be^{-t/\tau} = C(1 - e^{-t/\tau}) \quad (3)$$

where B has been selected so that the membrane is initially at zero concentration. Substitution into the differential equation gives τ:

$$\frac{AD}{l} Be^{-t/\tau} = \frac{VKB}{\tau} e^{-t/\tau} \quad \text{or} \quad \tau = \frac{VK}{ADl} \quad (4)$$

In the present case, $N_{[Pt(NH_3)_4]^{2+}}(t)$ is given by

$$N_{[Pt(NH_3)_4]^{2+}}(t) = \frac{2C^*_{[Pt(NH_3)_4]^{2+}}}{C^-}$$

where

$$C^*_{[Pt(NH_3)_4]^{2+}} = \frac{A}{V} \int_0^t D_{[Pt(NH_3)_4]^{2+}} \left. \frac{\partial C^*_{[Pt(NH_3)_4]^{2+}}}{\partial x} \right|_{x=l} dt \quad (5)$$

In deriving Equation 5, the following hypotheses have been made: (i) the platinum concentration in the solution being limited to ca. 5×10^{-2} M by the solubility of the salt at room temperature, it is assumed that the chloride co-ions are excluded from the membrane (Donnan exclusion); (ii) the ionic concentrations in the bulk solution are assumed to remain unchanged (infinite volume of solution and efficient stirring); (iii) the effect of the electric field on diffusion in the diffusion layer is negligible; (iv) it is assumed that the platinum concentration varies linearly with x across the diffusion layer (quasisteady state).

The thickness of the diffusion layer adherent to the membrane surface (l) is the only unknown in Equation 5. Its value can be estimated from mass transfer correlations [15]:

$$\frac{D}{l\nu} = 0.664 Re^{(-1/2)} Sc^{(-2/3)} \quad (6)$$

D is the diffusion coefficient of the diffusing species in the solution. Under the assumption of zero electric field in the diffusion layer, the value of $D_{[Pt(NH_3)_4]^{2+}}$ ($8.3 \times 10^{-6}\,cm^2\,s^{-1}$) was used to determine l from Equation 6.

Equation 6 pertains to a laminar flow parallel to the membrane surface. The relation can be used for Reynolds numbers smaller than 3×10^3. This is the case in the present experiments, where the Reynolds number is always lower than 1×10^3.

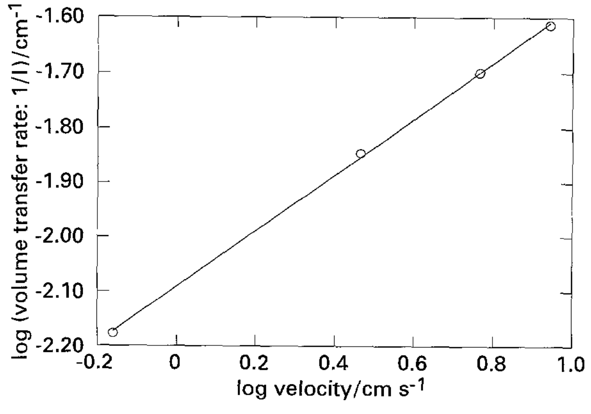

Fig. 7. Hydrodynamics at the membrane–solution interface. Log (mass transfer rate) against log (fluid velocity). [$y = -2.0908 + 0.51192x$; $Re = 0.99976$].

Figure 7 shows the linear relation between the mass transfer rate and the fluid velocity in the cell on a log scale. The proportionality to the power 0.5 is characteristic of laminar flow. Equation 6 can therefore be used for the determination of the thickness of the diffusion layer.

Data of Fig. 4(a) suggest that the L mechanism prevails only for low flow rates. With a flow rate of $0.083\,cm^2\,s^{-1}$, the thickness of the diffusion layer obtained from Equation 6 is 180 μm, that is twice the value of the membrane thickness (the membrane has a total thickness of 190 μm and is surrounded by two 180 μm thick diffusion layers).

3.3. *M mechanism*

Values of the diffusion coefficients for cationic species in Nafion® membrane are generally lower than those in aqueous solution, due to specific interactions between the diffusing species and the organic matrix [16]. Studies of Nafion® membranes have shown that its structure consists of two different phases [17]: (i) an organic fluorocarbon phase and (ii) hydrophilic microphase made of interconnected spherical clusters having an average diameter of a few nanometre. Ionic diffusion occurs across these clusters and the process of diffusion can be described as in any other isotropic medium.

If the M mechanism is rate-controlling, then the rate of exchange satisfies Fick's second law:

$$\frac{\partial C^*_{[Pt(NH_3)_4]^{2+}}}{\partial t} = D_{[Pt(NH_3)_4]^{2+}} \frac{\partial^2 C^*_{[Pt(NH_3)_4]^{2+}}}{\partial x^2} \quad (7)$$

In the case of a nonsteady state diffusion with uniform initial distribution and equal surface concentration, a semianalytical solution is given in [18]:

$$N_{[Pt(NH_3)_4]^{2+}}(t) = 1 - \sum_{j=0}^{\infty} \frac{8}{(2j+1)^2 \pi^2} \exp\left[-D_{[Pt(NH_3)_4]^{2+}} (2j+1)^2 \frac{\pi^2 t}{4l^2} \right] \quad (8)$$

In deriving Equation 8, the following hypotheses have been made: (i) the platinum concentration in the solution being limited to ca. 5×10^{-2} M by the solubility of the salt at room temperature, it is assumed that the chloride co-ions are excluded from the membrane (Donnan exclusion); (ii) the ionic concentrations in the bulk solution are assumed to remain unchanged (infinite volume of solution and efficient stirring); (iii) the effect of the electric field on diffusion in the membrane is negligible; (iv) the diffusion coefficient of the diffusing species is independent of concentration; (v) the ion-exchange equilibrium constant is assumed to be independent of $N_{[Pt(NH_3)_4]^{2+}}$ and to be independent of the flux at the interface [19].

In Equation 8, the rate of exchange is independent of the solution salt concentration and of the regime

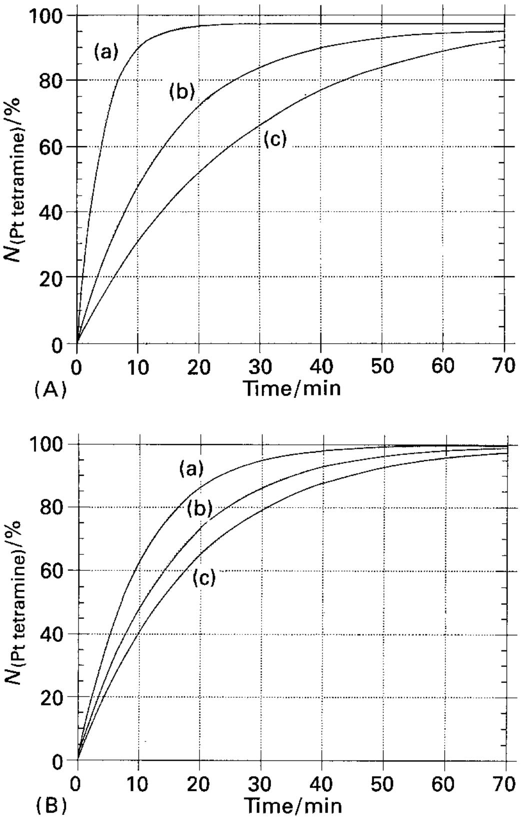

Fig. 8. $N_{[\mathrm{Pt(NH_3)_4}]^{2+}}$ (expressed in %) as a function of time; calculated graphs obtained (A) for different $[\mathrm{Pt(NH_3)_4}]^{2+}$ concentrations in the solution and with a layer thickness of 150 μm and (B) for different layer thicknesses and with a salt concentration of 10^{-2} M.

of stirring. Only D (the diffusion coefficient of the sorbing species) and l (the membrane thickness) play a role.

4. Results and discussion

4.1. *Solutions to the model*

Figure 8(A) and (B) are relative to an L mechanism. Figure 8(A) shows the time variation of $N_{[\mathrm{Pt(NH_3)_4}]^{2+}}$ for a number of different salt concentrations in the solution at constant diffusion layer thickness (150 μm). Figure 8(B) shows the time variation of $N_{[\mathrm{Pt(NH_3)_4}]^{2+}}$ for a number of different diffusion layer thicknesses at constant salt concentration (10^{-2} M). The influence of the salt concentration and the layer thickness on $t_{1/2}$ is clearly seen.

4.2. *Comparison of experimental and calculated data*

Results obtained for three different salt concentrations at constant flow rate (0.083 cm^3 s^{-1}) are shown in Fig. 9. The calculation in Fig. 9 used Equation 5 because the flow rate was below the point at which the ion exchange rate is independent of flow (Fig. 4(a)). The thickness of the diffusion layer used for the calculation was 180 μm, as indicated in Section 3.2. Results obtained for three different flow rates at constant salt concentration (10^{-2} M) are shown in Fig. 10. The calculation in Fig. 10 used Equation 8 because the flow rates were all above the point at which the ion-exchange rate is independent of flow.

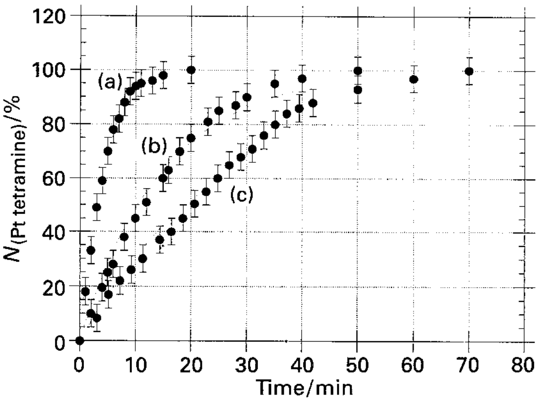

Fig. 9. $N_{[\mathrm{Pt(NH_3)_4}]^{2+}}$ (expressed in %) as a function of time; effect of the salt concentration at constant flow rate (0.083 cm^3 s^{-1}): (a) 3.75×10^{-2}, (b) 1×10^{-2} and (c) $5.5. \times 10^{-3}$ M. Calculated from Equation 5 with $l = 180\,\mu$m (···) and experimental (●) points.

A good agreement is found between the experimental and simulated results for both sets of experiments. This suggests that the rate of ion-exchange shifts from an L to an M controlled mechanism. This point is of particular importance for the preparation of large surface composites. By monitoring the ion-exchange conditions, it is possible to control the amount of platinum salt incorporated into the membrane and which can be deposited at the membrane surfaces. Care must be taken in designing plating cells in order to obtain homogeneous platinum sorption at the membrane surface.

However, since the platinum diffusion coefficient in the membrane is about 15 times slower than that in the solution and since the diffusion layer thickness is only twice the membrane thickness with a flow rate of 0.083 cm^3 s^{-1}, it is possible that the rate of ion exchange is controlled by a mixed (L–M) mechanism. Additional work is required to determine precisely which mechanism prevails for such flow rates.

5. Conclusions

By considering the two limiting sorption mechanisms, it has been possible to compute $N_{[\mathrm{Pt(NH_3)_4}]^{2+}}(t)$.

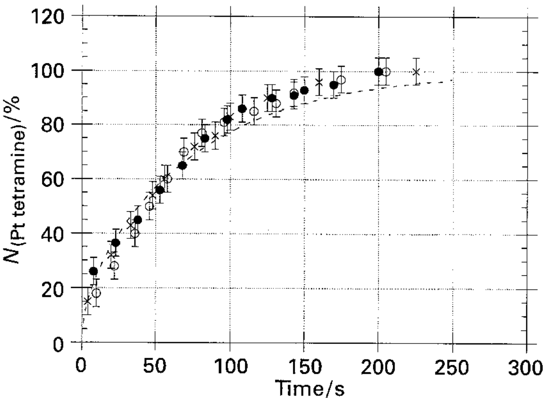

Fig. 10. $N_{[\mathrm{Pt(NH_3)_4}]^{2+}}$ (expressed in %) as a function of time; effect of flow rate at constant salt concentration (10^{-2} M): (a) 0.35, (b) 0.7 and (c) 1.05 cm^3 s^{-1}. Calculated from Equation 8 (···) and experimental (○, ●, ×) points.

Simulated values obtained correlate well with experimental data obtained *in situ* using EXAFS in dispersive mode. A change in the rate determining mechanism of ion-exchange is observed. This change is controlled by the salt concentration in the solution and the hydrodynamics at the membrane–solution interface.

The good correlation between experimental and calculated results suggests that the effect of the electric field on diffusion remains negligible during the ion-exchange process.

From a practical point of view, it is now possible to control the amount of platinum tetramine incorporated into the membrane for the preparation of platinum based MEAs. This point is of particular importance to limit the amount of platinum deposited (cost considerations) and to obtain homogeneous platinum deposits on large surface membranes.

This model also applies to two other cases of interest. First, the incorporation of a mixture of cations with various fractional concentrations. For example, we are currently investigating the *in situ* coreduction of platinum and ruthenium ions within Nafion® membranes. Ruthenium based anodes are interesting in that they allow lower anodic overvoltages (220 mV at 1 A cm^{-2} against 340 mV for platinum) but ruthenium is rapidly corroded [20]. Its coreduction with platinum may lead to more stable ruthenium-based anodes. The model can also be used to predict the rate of poisoning by metallic cations of the EME units of an electrolyser pilot plant. Circulation of highly deionised water (18 MΩ cm at 25 °C) in the stainless steel parts of an SPE® water electrolyser results in a slow and steady corrosion of the steel pipes. The concentration of various impurities (mainly Fe, Cu and Ni) slowly increases with time. Ion-exchange with the membranes of the cell stack leads to drastic losses in cell efficiency [21].

In a subsequent paper [22], results concerning the simulation of the precipitation process will be presented.

References

[1] 'Solid Polymer Electrolyte Water Electrolysis Technology Development for Large Scale Hydrogen Production', General Electric Company, DOE report DOE/ET/26 202-1 (1981).

[2] M. S. Wilson and S. Gottesfeld, *J. Electrochem. Soc.* **139** (1992) L-28.

[3] W. A. Titterington and J. F. Austin, Abstract 233, p. 576; The Electrochemical Society Extended Abstracts, vol. 74-2, New York, NY, 13–17 Oct. (1974).

[4] R. J. Lawrence and L. D. Wood, *US Patent 4 272 353*, 9 June (1981).

[5] H. Takenaka, E. Torikai, Y. Kawami and N. Wakabayashi, *Int. J. Hydrogen Energy* **7** (1982) 397.

[6] P. Millet, R. Durand and M. Pinéri, *J. Appl. Electrochem.* **19** (1989) 162.

[7] *Idem, Int. J. Hydrogen Energy* **15** (1990) 245.

[8] P. Millet, R. Durand, E. Dartyge, G. Tourillon and A. Fontaine, *J. Electrochem. Soc.* **140** (1993) 1373.

[9] R. Parsons, 'Handbook of Electrochemical Constants', Butterworths, London (1959).

[10] A. J. Bard, R. Parsons and J. Jordan, 'Standards Potentials in Aqueous Solutions', Marcel Dekker, New York (1985).

[11] A. J. Bard and J. Faulkner, 'Electrochemical Methods. Fundamentals and Applications', John Wiley, New York (1980).

[12] P. Millet, *J. Membrane Sci.* **50** (1990) 325.

[13] H. L. Yeager and A. Steck, *Anal. Chem.* **51** (1979) 862.

[14] T. R. E. Kressman and A. Kitchener, *J. Chem. Soc.* **91** (1949).

[15] C. O. Bennett and J. E. Myers, 'Momentum, Heat and Mass Transfer', MacGraw-Hill (1962) p. 476.

[16] A. Eisenberg and H. L. Yeager, 'Perfluorinated Ionomer Membranes'. Workshop on perfluorinated ionomer membranes, Lake Buena Vista, ACS Symposium Series, 180, American Chemical Society, Washington, DC (1982) p. 41.

[17] W. Y. Hsu and T. D. Gierke, *J. Membrane Sci.* **13** (1983) 307.

[18] J. Crank, 'The Mathematics of Diffusion', Oxford University Press, 2nd edn (1975) p. 48.

[19] C. Selvey and H. Reiss, *J. Membrane Sci.* **30** (1987) 75.

[20] S. Stucki and A. Menth, *in* Proceedings of the Symposium on Industrial Water Electrolysis, ECS Series (1978) p. 180.

[21] P. Millet, T. Alleau and R. Durand, *J. Appl. Electrochem.* **23** (1993) 322.

[22] P. Millet, F. Andolfatto and R. Durand, *J. Appl. Electrochem.*, submitted.